Computer aided control system design - Project I: seesaw

Pieter Vanslambrouck & Zander Op de Beeck

June 5, 2022

1 Model and open loop analysis

1.1 Linear state-space model

The state variables of the system are

x, the position of the cart on the rail in meters, where zero it the rail's centre and right is the positive direction.

θ, the angle of the seasaw in radians, where zero is the seesaw being level and counter-clockwise is the positive sense of rotation,

$\dot{x}$, the speed of the cart on the rail in meters per second and

$\dot{\theta}$, the angular velocity of the seesaw pivoting around its axis in radians per second.

This yields $\vec{x} = [x, \theta, \dot{x}, \dot{\theta}]^T$.

The linear state-space of the model can be found directly form the linearization of the global model provided in section 2.1.3 of the assignment text, and filling in the parameters.

We remark that there seems to be an error in the assignment. At the end of the pdf, J_{sw} is described as the moment of inertia of the seasaw about its center of gravity. However, in the formulas J_{sw} is used as the moment of inertia about the pivot point (which does not coincide with the center of gravity of the seesaw). We have assumed that the numerical value given for J_{sw} is the moment of inertia about the pivot point and have proceeded with the given formulas.

The system matrix is

$$A = \begin{bmatrix} 0 & 0 & 1 & 0 \\ 0 & 0 & 0 & 1 \\ -1.6143 & -9.1618 & -16.9249 & 0 \\ -12.9144 & 5.1856 & -2.7290 & 0 \end{bmatrix}.$$

The top-right block of four values is a direct consequence of the derivatives of variables being explicitly present as model parameters; for the model to satisfy $\dot{x} = \dot{x}$ and $\dot{\theta} = \dot{\theta}$, which everything always should, the entire top two rows of A should be as they are, and the top two values in B should be zero.

The zero values in the bottom right corner and the place above it are a direct consequence of ignoring the friction on the pivot by choosing $B_{sw} = 0$, hence, the model predicts no influence of the speed of rotation on the acceleration of the cart or the rotation itself.

The rest of the values provide the nonzero forces in the system (per unit of mass), giving the accelerations in accordance with classical mechanics and then linearized, as elaborately discribed in the assignment text.

The input matrix is

$$B = \begin{bmatrix} 0 \\ 0 \\ 3.3827 \\ 0.5454 \end{bmatrix}.$$

No direct manipulation of the position of the cart and seesaw itself is possible, resulting in te zeros in the top two spots of this matrix. While only the acceleration of the cart can be directly controlled by supplying voltage, this instantaneously creates a rotational acceleration of the seesaw around its pivot point as well.

The output matrix usually is

$$C = \begin{bmatrix} 1 & 0 & 0 & 0 \\ 0 & 1 & 0 & 0 \end{bmatrix},$$

as the output $\vec{y}$ is taken to be $[x, \theta]^T$. In absence of direct knowedge of the derivatives, these can be approximated using, for example, backwards differences (for which a filter is needed), as will be discussed further. In some parts of the project, the entire state $\vec{x} = [x, \theta, \dot{x}, \dot{\theta}]^T$ is considered known, in which case C is a 4×4 idenity matrix.

The direct transmission matrix is

$$D = \begin{bmatrix} 0 \\ 0 \end{bmatrix},$$

as no direct connection from the input to the output is made.

1.2 Open loop analysis

As can be seen in figure 1, the open-loop system has poles in the following four locations: -16.7635, 2.9006 and $-1.5310 \pm 0.5114i$.

As D, being non-square, is not invertible, transmission zeros cannot be found using the eigenvalues of $A - BD^{-1}C$, yet the matlab command `tzero` yields no invariant zeros, which are a superset of the transmission zeros, hence no transmission zeros.

The eigenvalues of the system matrix are the same as the poles, one (> 0) of which has a real part greater than zero, making the (continuous) system unstable.

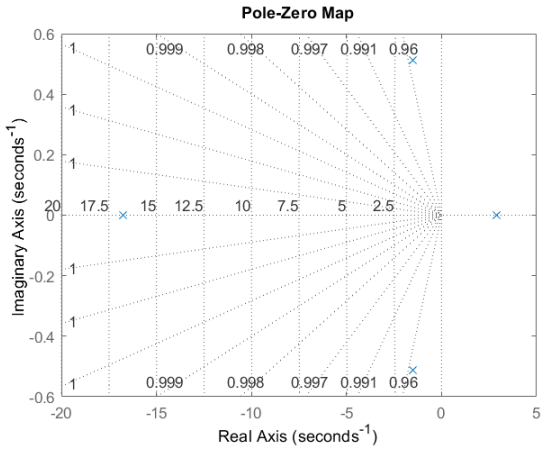

Figure 1: Pole-zero map of the open-loop system.

The controllability matrix can be found to be

$$\begin{pmatrix} 0 & 0.0003 & -0.0057 & 0.0959 \\ 0 & 0.0001 & -0.0009 & 0.0115 \\ 0.0003 & -0.0057 & 0.0959 & -1.6046 \\ 0.0001 & -0.0009 & 0.0115 & -0.1924 \end{pmatrix} \times 10^4,$$

which has rank four, proving it to be of full rank and hence proving the system to be controllable.

Similarly, the observability matrix can be found to be

$$\begin{pmatrix} 1.0000 & 0 & 0 & 0 \\ 1.0000 & 0 & 0 & 0 \\ 0 & 0 & 1.0000 & 0 \\ 0 & 0 & 0 & 1.0000 \\ -1.6143 & -9.1618 & -16.9249 & 0 \\ -12.9144 & 5.1856 & -2.7290 & 0 \\ 27.3219 & 155.0625 & 284.8379 & -9.1618 \\ 4.4054 & 25.0023 & 33.2732 & 5.1856 \end{pmatrix},$$

which has rank four as well, meaning it is full-rank, meaning the system is observable.

As the system is controllable, every unstable mode can be controlled, making it stabilizable.

The system is observable, so all unstable modes are observable as well, implying the system to be detectable.

As system is controllable and observable, it is minimal.

1.3 Control goals

For the control goals, closed loop eigenvalues as well as the step response will be used. Of course, the eigenvalues must prove the system to be stable, but as an additional requirement the dominant poles should have a real part of at most -3. Furthermore, we require the distance on the real axis between the dominant pair of poles and the next-dominant one(s) to be at least one. This is done to keep the behaviour of the system close to the second-order system corresponding to the dominant pair of poles.

As for the step response, the over- and-undershoot are to be less than 0.01 rad, and the settling time less than two seconds.

2 Design of the LQR controller and creation of the first closed-loop simulation diagram

2.1 Simulink diagram

An image of the simulink diagram for the fists open-loop system can be found in figure 2. It directly refers to and depends on a file `closed_loop1.m`, which contains the parameters to be set and in turn depends on `main.m`, laying out the overall structure.

The desired value for x can be found as a function of the desired value for θ, which is implemented in `get_x_desired`. The difference of the desired x and *theta* –the error– is calculated using the two sum blocks an fed, through a multiplication $-K$, the negative of the state-feedback gain. This, added to the reference voltage, yields

$$-K(x - x_{ref}) + u_{ref},$$

as the input to the linearized model.

This model itself is the same global model as discussed in section 1, and provides a proxy for the real system to be controlled.

The control system to be designed, thus, resides in K.

2.2 Finding Q and R

As, for the optimization of the quadratic performance index

$$J = \int \vec{x}^T Q\vec{x} + \vec{u}^T R\vec{u}dt$$

only the relative sizes of Q and R with respect to eachother matter, R might as well be taken to be 1, leaving only Q to be optimized.

As Q is to be a diagonal matrix, this leaves only four parameters to optimise. The lower two of which relate to $\dot{x}$ and $\dot{\theta}$; differential action. These parameters are rather dangerous to play with; depending on their signs, either they encourage the movement in x and θ to speed up as it gets faster, which could easily lead to a runaway exponential growth wherein the controller tries merely to maximise the speed of the cart, or it would work as a break trying to limit the speed of movement, which would make the controller less aggressive. In light of these considerations, and after some experimentation (discussed below) confirming the controller wasn't overly aggressive, these parameters of Q were decided to be left at zero. A more rigorous search might have found better parameters including mixing terms, that might slow down the controller as the system gets closer to the desired configuration.

This leaves the upper two diagonal elements, working on x and θ themselves.

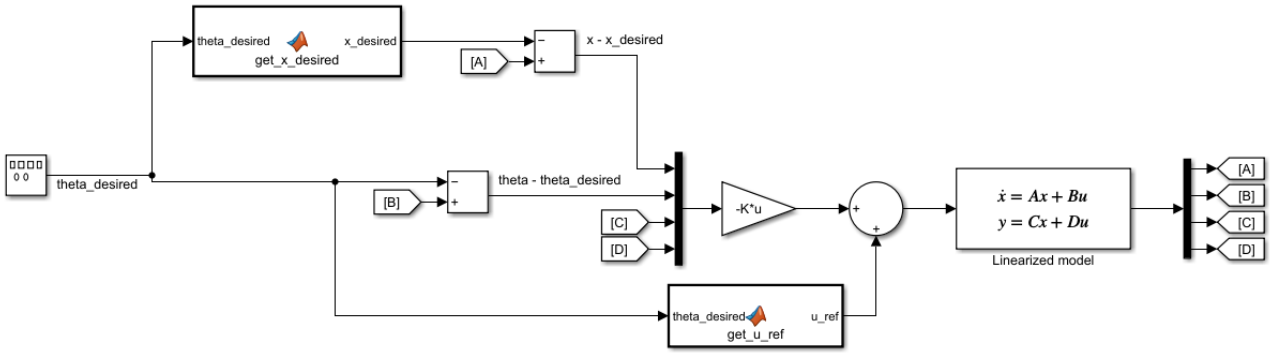

Figure 2: Simulink diagram for the first closed-loop system.

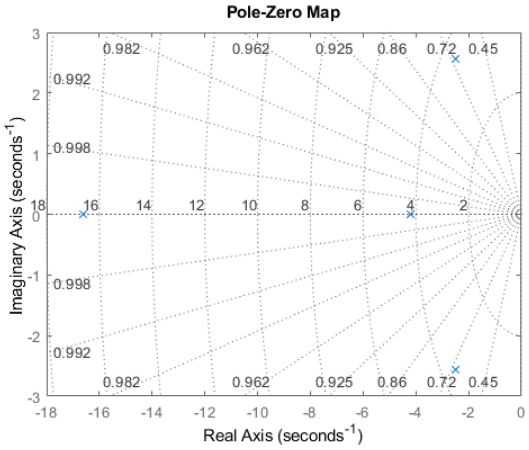

Figure 3: Pole-zero map for the first closed-loop LQR system using the given parameters.

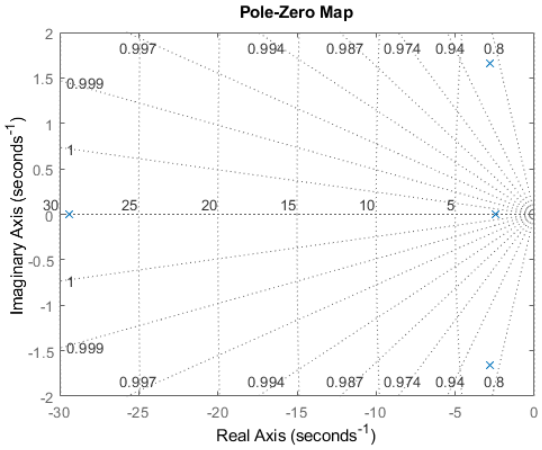

Figure 4: Pole-zero map for the first open-loop LQR system using the parameters of the first try.

Given parameters The given Q and R did not perform terribly, and provide a good starting point. It had the following poles: -16.6331, $-2.5056 \pm 2.5630i$ and -4.1851. While stable, the real part of the dominant pair is higher than desired. Besides, as can be seen on figure 3, the distance between the dominant pair and the pole at -4.1851 is rather small, causing the system to behave significantly different from a second-order system.

On figure 6, the step response of the initial parameters can be seen to have slightly too long of a settling time to meet the requirements, even if the overshoot falls well within the prescribed margin.

First major iteration Our first major iteration, thus, did indeed involve the lowermost diagonal terms of Q, setting the both to fifty, and setting the first two elements on the diagonal to fifty and three hundred, for $R = 1$. This resulted in the poles -29.4002, $-2.7923 \pm 1.6600i$ and -2.4782 as can be seen on figure 4. We hoped this configuration would dampen the dynamics a bit, and while the real part of the dominant pair is slightly lower, whatever good this did was completely offset by the fact that there was virtually no difference between the real part of the dominant pair and the following pole.

On figure 7, the step response of this iteration can be seen to exhibit less overshoot, yet the settling time is worse than before.

Final parameters Finally, we tried setting the two lowermost diagonal terms of Q to zero, as discussed before, and taking the first two to be four hundred and two thousand four hundred. The poles are now -16.1929, $-3.5423 \pm 3.4289i$ and -5.4593, meeting our design requirements and providing an acceptable margin between the dominant pair and the rest. A pole-zero–polt of these can be found in figure 5.

On figure 8, the step response of the final iteration can be seen to meet the desired specifications.

2.3 Change of setpoint

As the instructions mention the setpoint should be kept between minus two and two degrees, it was decided to model the setpoint spanning this whole range, as can be seen in figure 9.

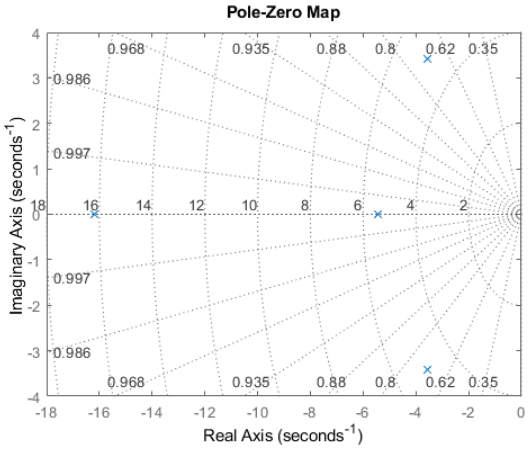

Figure 5: Pole-zero map for the first closed-loop LQR system using the final parameters.

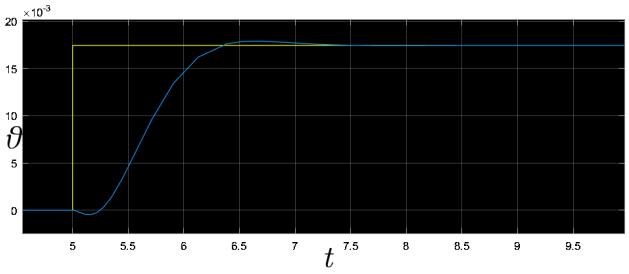

Figure 6: Step response for the initial given parameters. The desired θ is in yellow, and the actual θ in blue. In radians.

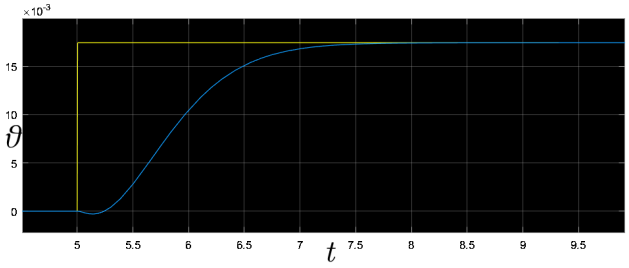

Figure 7: Step response for the first major iteration. The desired θ is in yellow, and the actual θ in blue. In radians.

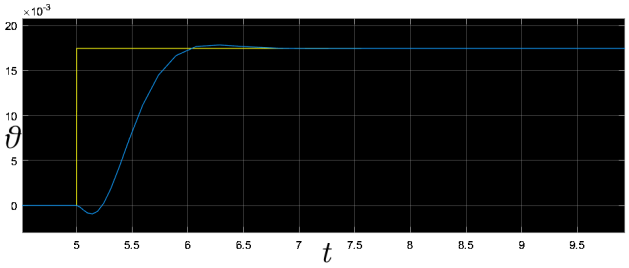

Figure 8: Step response for the final parameters. The desired θ is in yellow, and the actual θ in blue. In radians.

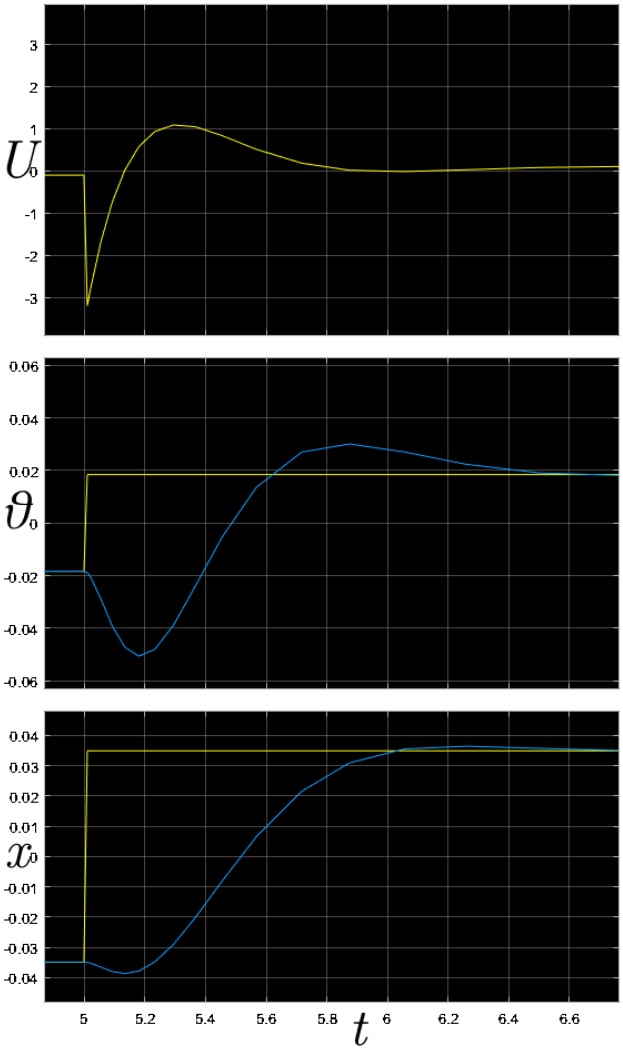

Figure 9: Setpoint change for the first closed-loop system. From top to bottom: the control action, the angle (blue) and its setpoint (yellow) and the position (blue) and its setpoint (yellow). Control action in volts, angle in radians and distance in metres.

3 Creation of the second closed-loop simulation diagram

3.1 Simulink diagram

The simulink diagram of the second closed-loop system can be found in figure 10. In the upper part, the desired value for θ is generated and fed trough the same functions as in the previous model for finding the desired x position and computing the control input. The difference between the desired and measured values for x and θ, however, cannot be done as straightforwardly as before; so as not to make the controller act on every single noise fluctuation, the measured values of x and θ are filterd using the

$$\frac{\beta}{1+(\beta-1)z^{-1}}$$

block. This is the low-pass filter where

$$\beta = \frac{\omega_c T_s}{1+\omega_c T_s}$$

with ω_c is the cutoff frequency and T_s the sampling time. These parameters are set in a separate script called `closed_loop2.m`. The cutoff frequency is set relatively high to $f_c = 10$ Hz to avoid slowing down the controller. T_s was set to 0.005s. The error values are then through the same LQR-controller contained in K as before, together with estimates for $\dot{x}$ and $\dot{\theta}$, found using a finite-difference formula as can be seen in the

$$\frac{1-z^{-1}}{T_s}$$

blocks in the two detached diagrams at the very bottom. As these estimates are found using measured data of x and θ, it makes sense to filter first using he same low-pass filter described previously, but allowing for the use of a different cutoff frequency incorporated in the parameter α. In fact, taking a numerical derivative of a noisy signal greatly amplifies this noise, so it makes sense to take a lower cutoff frequency to negate this effect.

The control signal is now fed through a saturation block, mapping any voltages between -3.5 V and 3.5 V to themselves, and any lower or higher voltages to their respective limits, as described in the assignment. The resulting voltage is fed into the linearized model of the seesaw itself, like in the previous part.

As the controller is digital, a quantisation of the noisy signal has to be made. The assignment text provides what ranges of voltages corresponded to what ranges of x positions and θ angles, as well as the resolution being ten bits. As ten bits can represent 2^{10} numbers, and the map is linear, the voltage would move in steps of 3.052×10^{-4} V, the distance 0.103 meter per volt and the angle 0.0827 radians per volt. Multiplying these numbers by the ones for the voltage yields 3.1556×10^{-5} and 2.5235×10^{-5} a the quantisation interval for x and θ respectively. It should be noted that if the measurement noise is smaller than half the distance between these intervals, it will be mostly filtered out by this procedure.

The outputs of the linear model is fed into zero-order hold digital-to-analogue converters, providing a signal suitable for the noise to be added to. There are two different noise blocks, so different amounts of noise can be added to both readings. The size of the noise can be determined experimentally - just let the setup run for a while sitting still, without providing any control whatsoever. If the quantisation did not filter it out, the distribution around the mean of the measurement will be the noise measurement. As the relationship guarding the distance or angle and the voltage is known, this can easily be converted back into noise on the voltage. The noise both on the angle and position turned out have a standard deviation of about 7.5×10^{-5}. As both the number of radians swept and the distance in meters traversed per voltage are about 0.1, it makes sense for these measurements to be very similar as it can be argued that the electrical equipment the noise stems from is largely shared, yielding similar noise levels.

3.2 Setpoint change

The same step change as before for the second, noisy closed-loop system can be seen in figure 11. Aside from the noise and the control actions being a bit less sharp because of that, the system behaves pretty much identically to the setup without noise. R and Q can thus be kept.

3.3 The role of the cutoff frequency

Setting the cutoff frequency too low causes the system too be a lot less noisy, but filters out a lot of the faster, non-noise information as well. This causes the controller to be slower (there is less "fast information" to act upon) and oscillate greatly, as can be seen in figure 12.

Setting the cutoff frequency too high, as in figure 13, causes a lot of noise to be visible in the control input, but it leaves the outputs mostly intact. The noise being high-frequency can be thought of as being averaged out by the slowness of the system, and as the noise is unbiased, this average is the desired control action.

In general, thus, it seems better to leave a bit of noise in than to remove too much signal.

4 Experimental results

4.1 Simulink diagram

The simulink diagram used for the experimental setup can be found in figure 14. It is identical to the one used for the second closed-loop system, except that the modelled system (including artificial noise) is now replaced by the real experimental setup. As a safety feature, the control can be turned on of of while running by

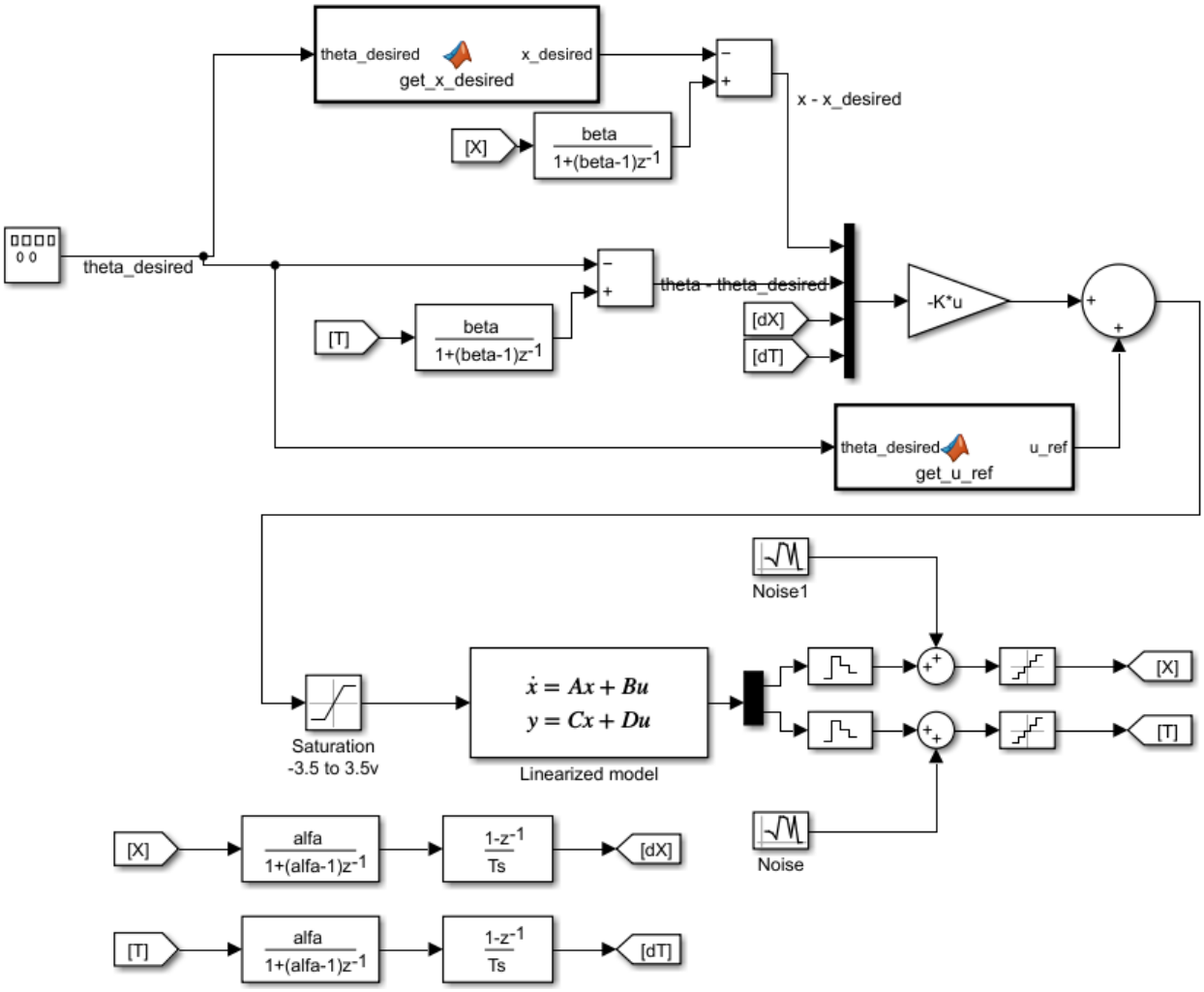

Figure 10: Simulink diagram of the second closed-loop system.

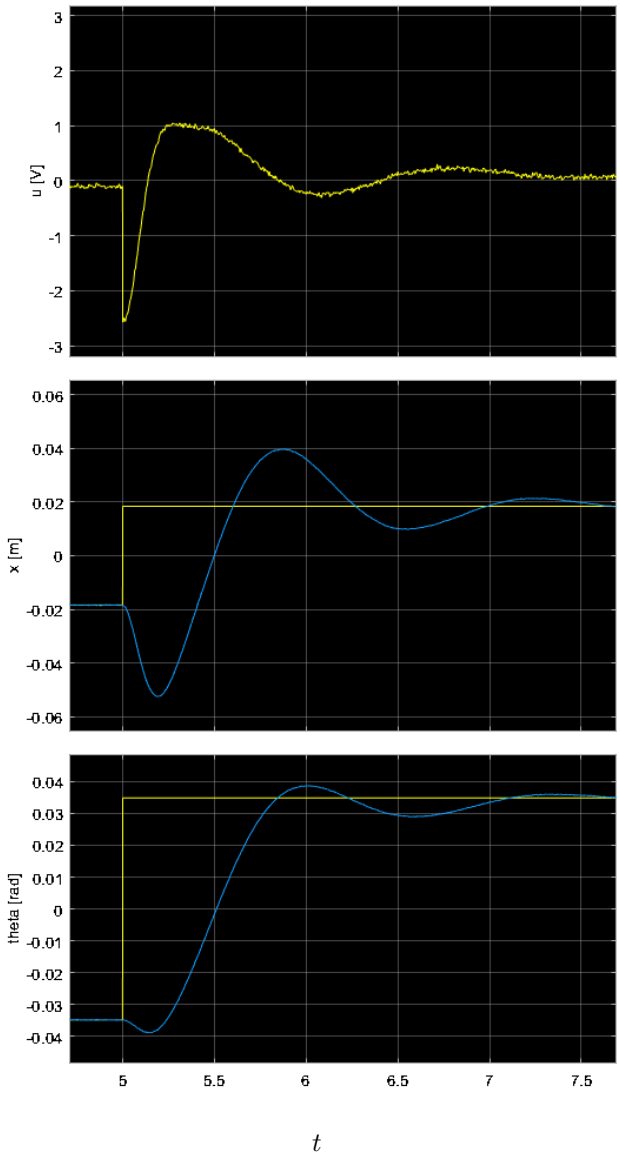

Figure 11: Setpoint change in θ for the second closed-loop system. From top to bottom: the control action, the angle (blue) and its setpoint (yellow) and the position (blue) and its setpoint (yellow).

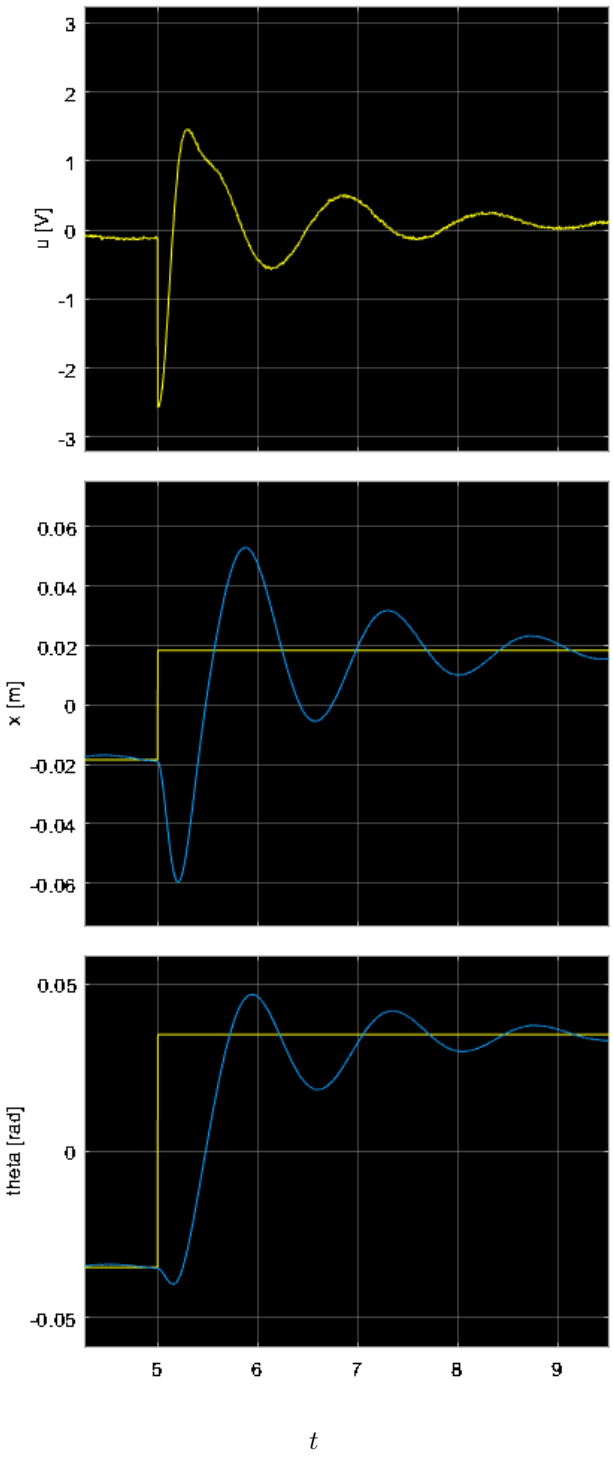

Figure 12: Setpoint change for the second closed-loop system, with a cutoff frequency of one hertz. From top to bottom: the control action, the angle (blue) and its setpoint (yellow) and the position (blue) and its setpoint (yellow).

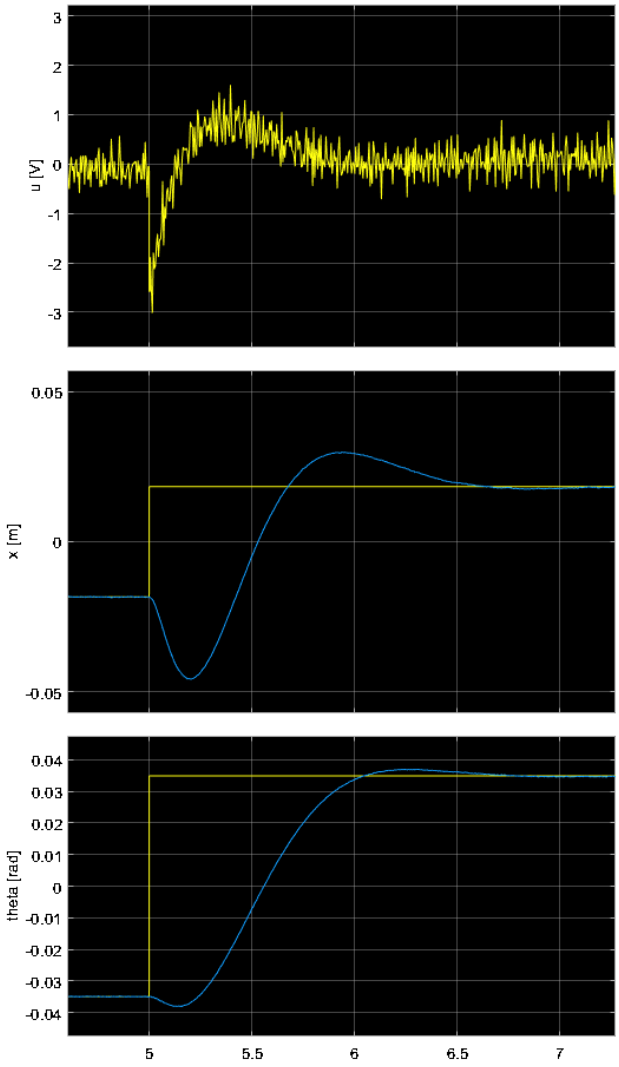

Figure 13: Setpoint change in θ for the second closed-loop system, with a cutoff frequency of forty. From top to bottom: the control action, the angle (blue) and its setpoint (yellow) and the position (blue) and its setpoint (yellow).

toggling the gate in the top right. The displays allow for easy calibration of the system (to do so, control is turned of and the system is held still by hand).

4.2 Retuning

As the Q matrix determined in the previous section[1] did not perform very well, to new Q-matrices were chosen and analysed separately. These matrices carry the names Q_0 and Q_1.

$$Q_0 = \begin{bmatrix} 400 & 0 & 0 & 0 \\ 0 & 2000 & 0 & 0 \\ 0 & 0 & 0 & 0 \\ 0 & 0 & 0 & 0 \end{bmatrix}$$

$$Q_1 = \begin{bmatrix} 800 & 0 & 0 & 0 \\ 0 & 5000 & 0 & 0 \\ 0 & 0 & 0 & 0 \\ 0 & 0 & 0 & 0 \end{bmatrix}$$

These parameters are not perfect, which is why there are two of them to compare. In both, the original structure of only filling in the two upper elements of the diagonal was retained, but the controller was made a little less aggressive in Q_1 and a lot more aggressive in Q_2.

4.3 Setpoint tracking tests

Plots of various setpoint tracking tests of the real system can be found in figures 15 through 22. In general, the results are much less neat than the ones obtained in the second, completely simulated closed-loop system, despite modelling the same thing. Even when the seesaw is to be held steady for an extended period of time, large oscillations occur reminiscent of what happened when too much of the signal was filtered away by the low-pass filter, even though this filter was set to the recommended cutoff frequency. Not even the the means of these oscillations line up with the desired values. As can be expected, these oscillations can be seen to be performed faster using the more aggressive Q_1, though the amplitude remains similar. Several reasons might explain these oscillations:

- Incorrect calibration (though this was checked very thoroughly).
- The controller might be too aggressive, though of the two controllers discussed here, the less aggressive Q_0 performs about as well as Q_1.
- The driving of the motor might not be as linear as expected; during the experiments, we had a hard time getting the cart to move slowly and, as can be seen in the video's, the cart accelerates very fast. We tried to remedy this using the lower two terms in Q, but, alas, to no avail. For a motor to start spinning it must overcome the static friction. When this is done, the motor is immediately presented with a lower sliding friction,

[1] We chose `Q = diag([400 2400 0 0])`.

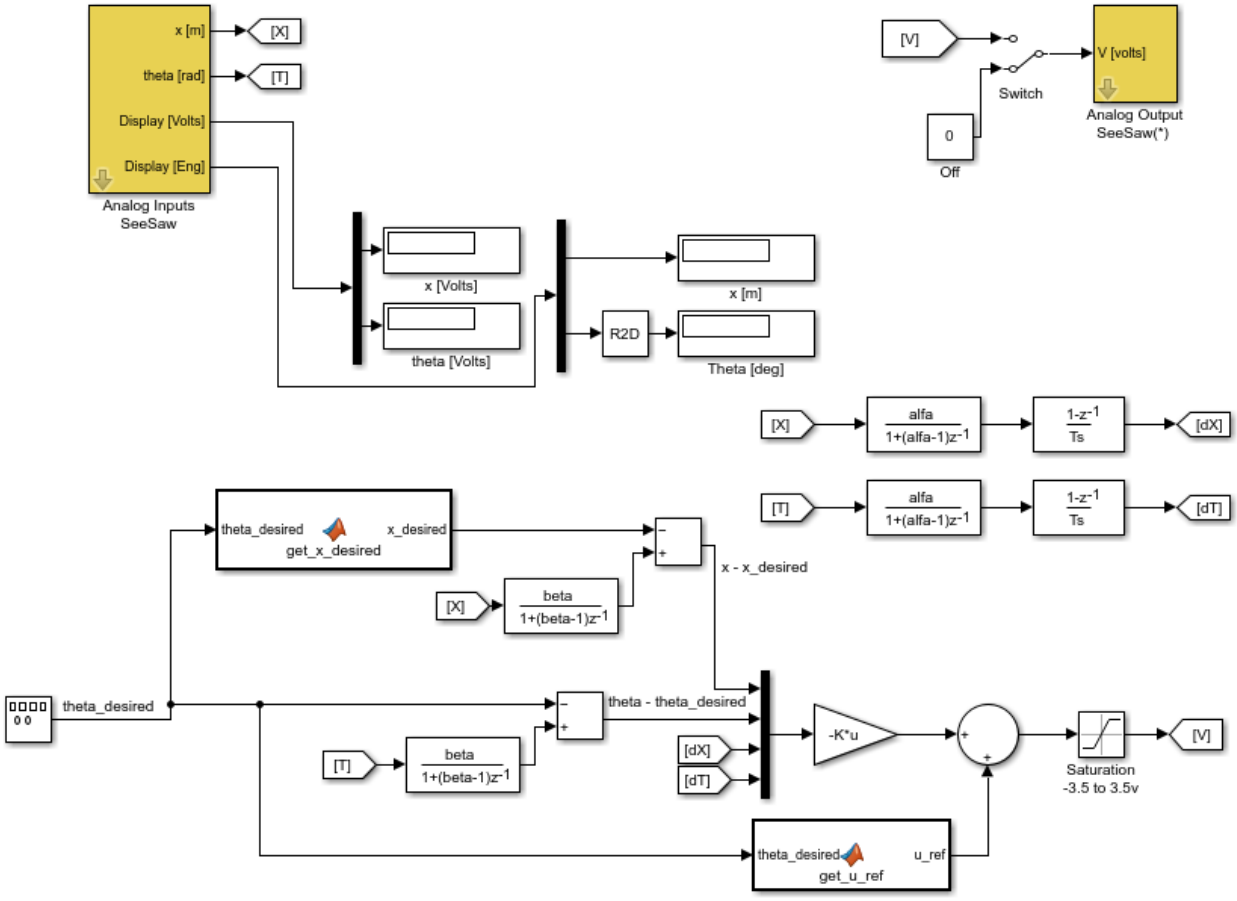

Figure 14: Simulink diagram of the experimental setup.

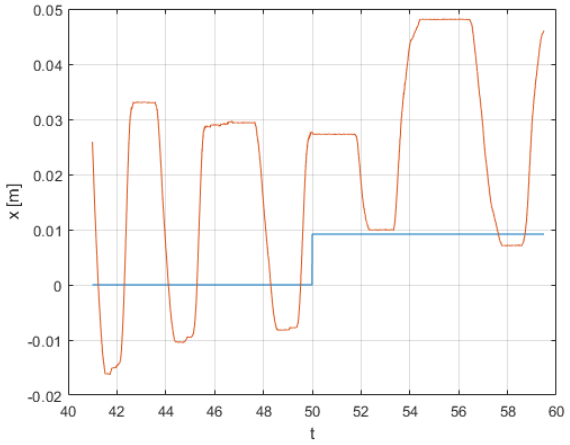

Figure 15: Step response of the real system to a change in desired θ from 0° to 1° using Q_0, x-value. The desired value is in blue, the measured one in orange.

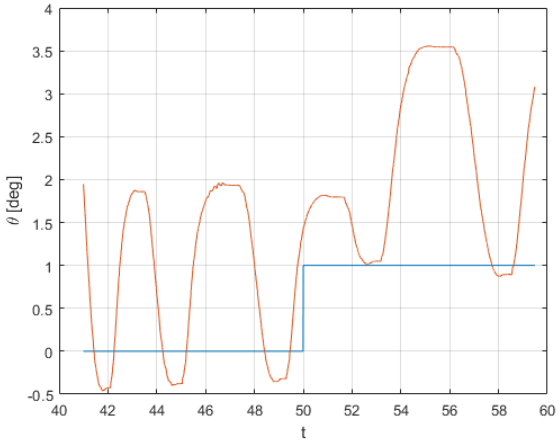

Figure 16: Step response of the real system to a change in desired θ from 0° to 1° using Q_0, θ-value. The desired value is in blue, the measured one in orange.

resulting in great acceleration. This phenomenon was not modelled, and might be (partly) responsible for the jagged motion of the cart. The cart regularly coming to a halt means this phenomenon occurs a lot. It also does not help that as the static friction is being overcome, the seesaw tilts further, causing the control system to supply the motor with even more power to be released in an instant when friction is overcome.

This second explanation might (in part) explain the large steady-state error in the plots; if the cart must move in fast jumps of a minimum length, the centre of gravity can only very suddenly be moved a while away, making small adjustments impossible. I.e. there is a (soft) minimum distance the cart must travel, which in turn forces every adjustment of the system either to be larger than some soft minimum. When balance is lost, thus, the controller can only wait for the problem to get worse until it has gotten so bad this relatively large "minimum action" would do more good than harm. And that is assuming a controller aware of this problem, which the implemented controller is not. The implemented controller will try to make the desired small adjustment, only for nothing to happen as the static friction is not overcome, and keep increasing the voltage until finally one of the steps is made, causing the imbalance the other way around and starting the whole cycle over. As long as this "minimum stepsize" is too large (and the cart doesn't end up exactly on the ideal spot by accident), the ideal spot simply cannot be reached, forcing the controller to use this infinite oscillation.

4.4 Disturbance rejection tests

Some disturbance rejection plots can be found in figures 23 and 24. The controller being as aggressive as it is, it manages to quickly recover from the disturbances, only to resettle in its previous oscillation. There is very little overshoot.

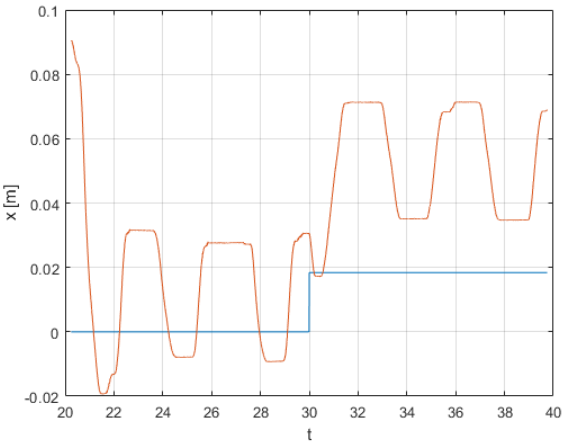

Figure 17: Setpoint change of the desired θ going from 0° to 2°, x-value using Q_0, x-value. The desired value is in blue, the measured one in orange.

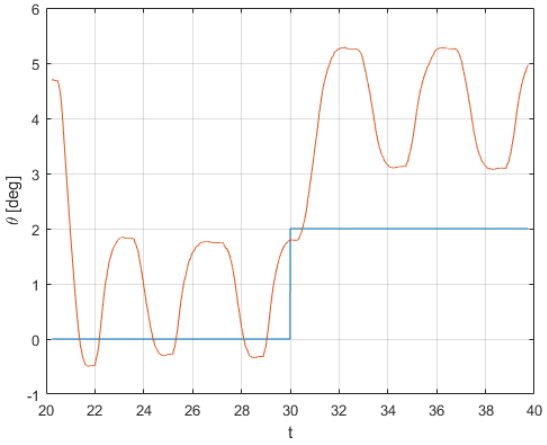

Figure 18: Setpoint change of the desired θ going from 0° to 2° using Q_0, θ-value. The desired value is in blue, the measured one in orange.

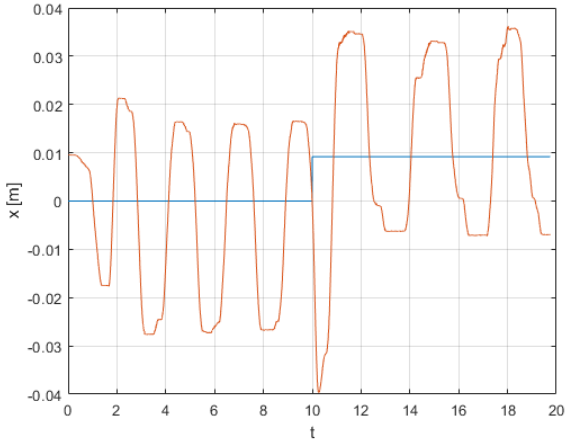

Figure 19: Step response of the real system to a change in desired θ from 0° to 1° using Q_1, θ-value. The desired value is in blue, the measured one in orange.

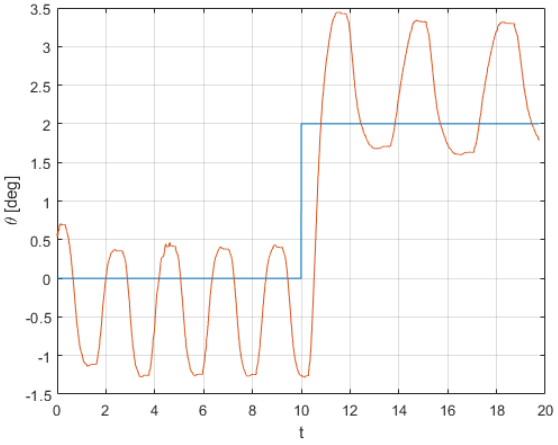

Figure 22: Setpoint change of the desired θ going from 0° to 2° using Q_1, θ-value. The desired value is in blue, the measured one in orange.

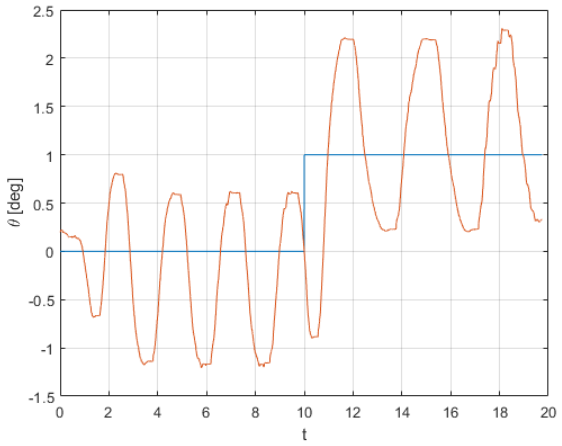

Figure 20: Step response of the real system to a change in desired θ from 0° to 1° using Q_1, θ-value. The desired value is in blue, the measured one in orange.

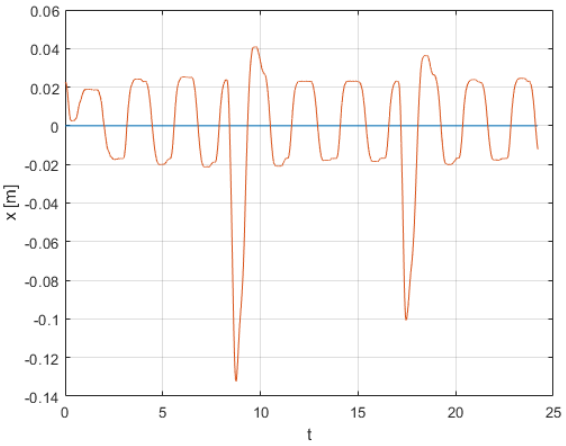

Figure 23: Experimental disturbance rejection tests using Q_1, x. The desired value is in blue, the measured one in orange. The disturbances are clearly visible.

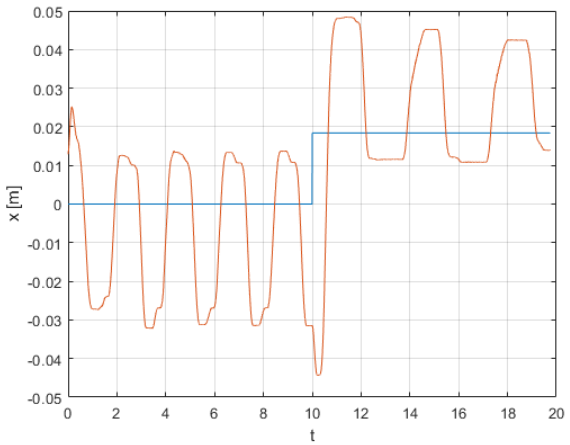

Figure 21: Setpoint change of the desired θ going from 0° to 2° using Q_1, x-value. The desired value is in blue, the measured one in orange.

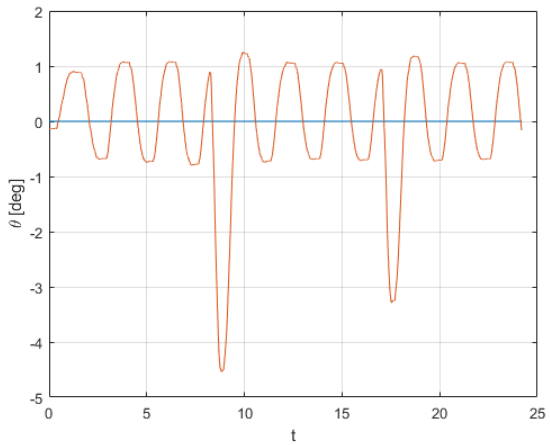

Figure 24: Experimental disturbance rejection tests using Q_1, θ. The desired value is in blue, the measured one in orange. The disturbances are clearly visible.

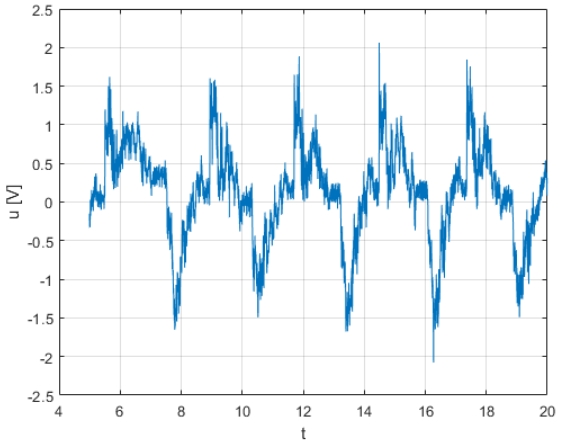

Figure 25: Control signal for the system of figure 26, where the cutoff frequency was set to eight hertz.

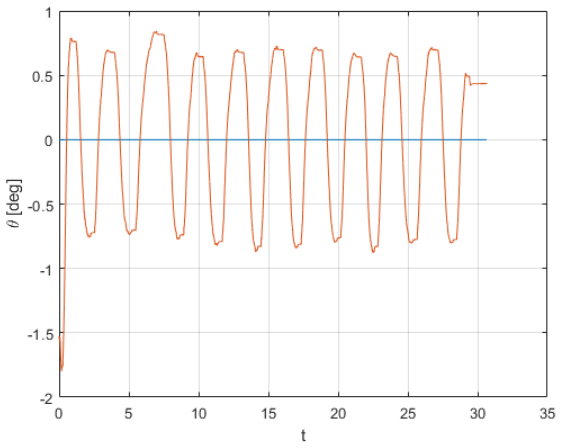

Figure 26: Angle of the seesaw to be kept at zero, where the cutoff frequency was set to eight hertz. The desired value is in blue, the measured one in orange.

4.5 Influence of the cutoff frequency

Figures 25 through 27 illustrate the the influence of the cutoff frequency. The same principles as for simulated system seem to apply; a cutoff frequency that is too high results in a very noisy control signal, but is ultimately less of a problem than setting it too low, which results in a significant increase in the amplitude of the oscillations.

4.6 Videos

Some videos were provided together with the rest of the files.

- `demo_equilibrium_with_disturbance.mp4`: the setpoint is equal to 0 degrees and we apply small disturbances.
- `demo_square_wave_amplitude_2deg.mp4`: the setpoint is a square wave that switches between a setpoint of +2 and -2 degrees with a period of 10 seconds.

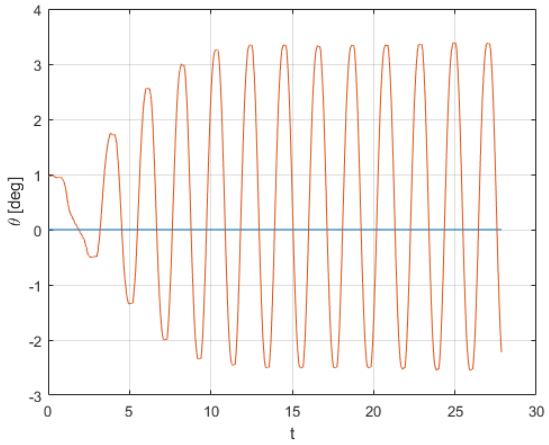

Figure 27: Angle of the seesaw to be kept at zero, where the cutoff frequency was set to 0.2 Hz. The desired value is in blue, the measured one in orange.

5 Conclusions

Considering the informal method used in designing the controller, barring oscillations, the system performed reasonably well. Doing this project, in combination with the plentiful examples discussed in the lectures gave us the impression that often, finding an adequate control system is doable relatively easily, but finding a perfect control system is very hard. The control system we found in the end is one of these easy ones; the seesaw doesn't touch the floor and it can recover from disturbances rather well, but the oscillations turned out to be a nuisance that was very hard to reduce and we did not manage to eliminate entirely.